Antiferromagnetic Interactions in Charge-Transfer Salts of Molybdocene Dithiolene Complexes: The Example of [Cp_2Mo(dddt)][TCNQ]

Marc Fourmigué,*,† Christine Lenoir,† Claude Coulon,‡ Fabrice Guyon,§ and Jacques Amaudrut*,§

Laboratoire de Physique des Solides (UA CNRS 02), Université Paris-Sud, 91405 Orsay, France, Centre de Recherche Paul Pascal, CNRS, Avenue Dr. Schweitzer, 33600 Pessac, France, and Laboratoire des Organométalliques, Université de Franche-Comté, 25030 Besançon, France

Received April 18, 1995[⊗]

Cp_2Mo^{IV}(dithiolene) complexes are prepared by reaction of Cp_2MoCl_2 with the dithiolene ligands $dmit^{2-}$ (2-thioxo-1,3-dithiole-4,5-dithiolate), $dmio^{2-}$ (2-oxo-1,3-dithiole-4,5-dithiolate), or $dddt^{2-}$ (5,6-dihydro-1,4-dithiine-2,3-dithiolate). Two reversible oxidation waves are observed by cyclic voltammetry for each complex. Cp_2Mo(dddt) crystallizes in the orthorhombic system, S. G. $Pna2_1$, with $a = 16.608(3)$ Å, $b = 11.568(2)$ Å, $c = 7.724(1)$ Å, and $Z = 4$. The MoS_2C_2 plane is folded along the S–S axis by 13(1)°. Oxidation of Cp_2Mo(dddt) with TCNQ affords an insulating 1:1 salt which crystallizes in the triclinic system, S. G. $P\text{-}1$, with $a = 9.597(1)$ Å, $b = 10.543(4)$ Å, $c = 12.460(3)$ Å, $\alpha = 84.41(2)°$, $\beta = 80.94(2)°$, $\gamma = 89.41(2)°$. In the 17-electron $Cp_2Mo(dddt)^{\bullet+}$ cation, the MoS_2C_2 plane is now folded along the S–S axis by 32.3(2)°. Those distortions upon electron count are rationalized by extended Hückel calculations. The structure of [Cp_2Mo(dddt)][TCNQ] can be described as strongly dimerized $(TCNQ_2)^{2-}$ moieties separated by chains of alternatingly spaced $Cp_2Mo(dddt)^{\bullet+}$ cations. The latter exhibit one-dimensional [$J/k = -27 \pm 1$ K, $\alpha J = (0-0.2)J$] antiferromagnetic interactions, as deduced from the temperature variations of the magnetic susceptibility.

Introduction

Molecular solids exhibiting high electrical conductivity,[1,2] ferromagnetic[3,4] or antiferromagnetic[5a,b] ordering are currently the subject of intense research effort. Such macroscopic properties are very sensitive to *intermolecular* interactions,[5c] as evidenced by the numerous organic donor or acceptor molecules with an extended π-system prepared and assembled into structures with a variety of dimensionalities and peculiar electronic and magnetic properties. Paramagnetic metal complexes offer an attractive alternative to organic π-donor molecules for the elaboration of electroactive multidimensional networks. Thus, metal dithiolene complexes[6] such as the prototypical $Ni(dmit)_2^{x-}$ complexes[7] ($x = 2, 1, 0.33, 0$; $dmit^{2-}$ = 2-thioxo-1,3-dithiole-4,5-dithiolate) provide a successful example of this approach. In the latter the frontier orbitals of interest are mainly concentrated on the dithiolene ligands, and the electronic properties of those materials are largely dominated by intermolecular ligand–ligand interactions, unless the spatial expansion of the metal orbitals (d_{z^2} in Pt or Pd salts) can play a role, by protuding out of the ligand π-system.[8] More recently, *nonplanar* tris(dithiolene) metal complexes[9–11] of D_{3h} symmetry, such as $Mo(dmit)_3^{2-}$ or $V(dddt)_3^{1-}$, have been shown to also present attractive structural and electronic features, and several cation-radical salts have been reported. Another successful example of strongly interacting nonplanar metal complexes is provided by decamethylmetallocenes[3,4] which when engaged into charge-transfer salts with π-acceptors, exhibit ferromagnetic properties. The origin of bulk ferromagnetism in such molecular-based materials has been explained by several mechanisms involving ligand-centered molecular orbitals.[3,12,13]

Thus, one may expect paramagnetic metal complexes including both cyclopentadienyl *and* dithiolene ligands to form extended networks with strong electronic interactions. We were

† Université Paris-Sud. New permanent address: Institut des Matériaux (IMN), 2, Rue de la Houssinière, 44072 Nantes Cedex 03, France.
‡ Centre de Recherche Paul Pascal.
§ Université de Franche-Comté.
⊗ Abstract published in *Advance ACS Abstracts,* August 15, 1995.

(1) (a) Miller, J. S., Ed. *Extended Linear Chain Compounds*; Plenum: New York, 1982; Vols. 1–3. (b) Whangbo, M.-H. *Acc. Chem. Res.* **1983**, *16*, 95. (c) Williams, J. M.; Ferraro, J. R.; Thorn, R. J.; Carlson, K. D.; Geiser, U.; Wang, H. H.; Kini, A. M.; Whangbo, M.-H. *Organic Superconductors*; Prentice Hall: Englewood Cliffs, NJ, 1992.
(2) (a) Saito, G., Kagoshima, S., Eds.; *The Physics and Chemistry of Organic Superconductors*; Springer-Verlag: Berlin, 1990. (b) Hebard, A. F.; Rosseinsky, M. J.; Haddon, R. C.; Murphy, D. W.; Glarum, S. H.; Palstra, T. T. M.; Ramirez, A. P.; Kartan, A. R. *Nature* **1991**, *350*, 600.
(3) For a recent review, see: Miller, J. S., Epstein, A. J. *Angew. Chem., Int. Ed. Engl.* **1994**, *33*, 385.
(4) (a) Broderick, W. E.; Thompson, J. A.; Day, E. P.; Hoffman, B. M. *Science* **1990**, *249*, 401. (b) Broderick, W. E.; Hoffman, B. M. *J. Am. Chem. Soc.* **1991**, *113*, 6334.
(5) (a) Batail, P.; Livage, C.; Parkin, S. S. P.; Coulon, C.; Martin, J. D.; Canadell, E. *Angew. Chem., Intl. Ed. Engl.* **1991**, *30*, 1498. (b) Coulon, C.; Livage, C.; Gonzalvez, L.; Boubekeur, K.; Batail, P. *J. Phys. I France*, **1993**, *3*, 1153. (c) Fourmigué, M.; Batail, P. *Bull. Soc. Chim. Fr.* **1992**, *129*, 29.
(6) (a) Müller-Westerhoff, U. T.; Vance, B. In *Comprehensive Coordination Chemistry*; Wilkinson, S. G., Ed.; Pergamon Press: Oxford, U. K., 1982; Chapter 16-5, pp 595–631. (b) Cassoux, P.; Valade, L.; Kobayashi, H.; Kobayashi, A.; Clark, R. A.; Underhill, A. E. *Coord. Chem. Rev.* **1991**, *110*, 115. (c) Olk, R. M.; Olk, B.; Dietzsch, W.; Kirmse, R.; Hoyer, E. *Coord. Chem. Rev.* **1992**, *117*, 99.
(7) (a) Bousseau, M.; Valade, L.; Bruniquel, M. F.; Cassoux, P.; Garbauskas, M.; Interrante, L. V.; Kasper, K. *Nouv. J. Chim.* **1984**, *8*, 653. (b) Brossard, L.; Ribault, M.; Bousseau, M.; Valade, L.; Cassoux, P. *C. R. Acad. Sci., Ser. 2* **1986**, *302*, 205.
(8) (a) Canadell, E.; Rachidi, I. E.-I.; Ravy, S.; Pouget, J.-P.; Brossard, L.; Legros, J. P. *J. Phys. (Paris)* **1989**, *50*, 2967. (b) Canadell, E.; Ravy, S.; Pouget, J.-P.; Brossard, L. *Solid State Commun.* **1990**, *75*, 633.
(9) (a) Broderick, W. E.; McGhee, E. M.; Gofrey, M. R.; Hoffman, B. M.; Ibers, J. A. *Inorg. Chem.* **1989**, *28*, 2904. (b) Martin, J. D.; Canadell, E.; Batail, P. *Inorg. Chem.* **1992**, *31*, 3176.
(10) Livage, C.; Fourmigué, M.; Batail, P.; Canadell, E.; Coulon, C. *Bull. Soc. Chim. Fr.* **1993**, *130*, 761.
(11) Matsubayashi, G.; Douki, K.; Tamura, H.; Nakano, M.; Mori, W. *Inorg. Chem.* **1993**, *32*, 5990.
(12) McConnell, H. M. *J. Chem. Phys.* **1963**, *39*, 1910.
(13) (a) Kollmar, C.; Couty, M.; Kahn, O. *J. Am. Chem. Soc.* **1991**, *113*, 7994. (b) Kollmar, C.; Kahn, O. *J. Chem. Phys.* **1992**, *96*, 2988.

0020-1669/95/1334-4979$09.00/0

Chart 1

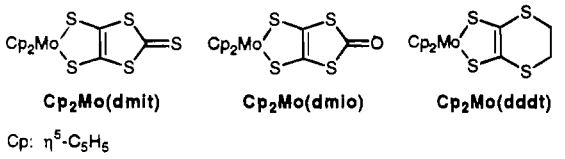

Chart 2

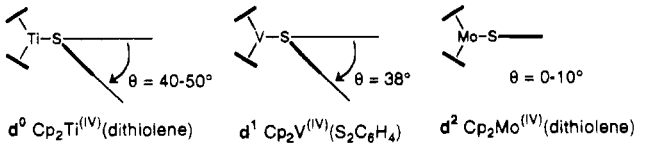

recently interested[14c] in such Ti^{IV} complexes of general formula Cp_2Ti(dithiolene) or $CpTi(dithiolene)_2^{1-}$. Those complexes are destroyed upon oxidation, however, indicating that the dithiolene ligands do not sufficiently stabilize the d^0 Ti^{IV} atom. Cp_2Nb^{IV}(dithiolene) complexes (d^1) were also investigated, and it was demonstrated that they do support reversible one-electron oxidation toward the d^0 Nb^V diamagnetic cations.[15] Thus, mixed cyclopentadienyl/dithiolene d^2 Mo^{IV} complexes of general formula *Cp_2Mo(dithiolene)* appear to be very promising candidates for the elaboration of functional materials. Several such complexes have been reported by Green with dithiolene ligands[16] such as o-$C_6H_4S_2^{2-}$ or $(CN)_2C_2S_2^{2-}$, and more recently a crown-ether-functionalized dithiolene complex was shown to exhibit reversible oxidations to the d^1 and d^0 species.[17] We have thus prepared and electrochemically characterized Cp_2Mo(dithiolene) complexes with electron-rich dithiolenes, such as $dmit^{2-}$, $dmio^{2-}$, or $dddt^{2-}$ ($dmio^{2-}$ = 2-oxo-1,3-dithiole-4,5-dithiolate; $dddt^{2-}$ = 5,6-dihydro-1,4-dithiine-2,3-dithiolate) (Chart 1).

Due to the large number of sulfur atoms at their periphery, those dithiolene ligands, when engaged in specific metal complexes, are expected to promote strong intermolecular interactions and thus to lead to extended networks of interesting conducting/magnetic properties.[5c] The ability of the dithiolene ligand to delocalize the paramagnetic center of 17-electron $Cp_2Mo(dithiolene)^{\bullet+}$ d^1 complexes is the key parameter for the setting of significant electronic interactions in the solid state. In short, can we describe the oxidation of the d^2 Cp_2Mo(dithiolene) complexes as a metal- or a ligand-centered process, or a mixture of both of them?

Also of interest in those complexes is the electron-count dependence of the geometry around the metal atom. In the analogous Ti(d^0) Cp_2Ti(dithiolene) complexes (Chart 2), the TiS_2C_2 plane is largely folded (up to 50°) along the S−S line.[14] Lauher and Hoffmann[18] have shown that, in these 16-electron complexes, the folding allows for an interaction of the π-orbital (b_1) of the dithiolene moiety with an empty Ti orbital (of a_1 symmetry in the unfolded (C_{2v}) conformation). Similarly, the 18-electron d^2 Cp_2Mo(dithiolene) complexes were predicted to be unfolded.

Scheme 1

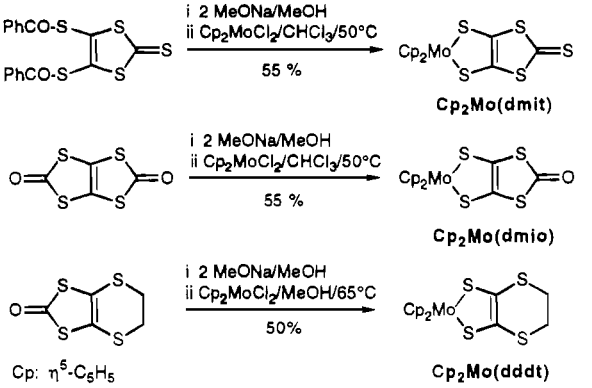

The intermediate situation of d^1 complexes is not well documented, and the synthesis and structural characterization of the d^1 vanadium complex $Cp_2V(o\text{-}S_2C_6H_4)$ in which the ligand plane is inclined at an intermediate angle value of 38.3° relative to the VS_2 plane was reported only recently.[19a] A similar distortion is observed in a Cp_2Nb(dmit) derivative.[19b] Such structural changes upon electron count are currently the focus of a large interest and have been investigated in electroactive organic[20] as well as organometallic[21] molecules. The Cp_2Mo(dithiolene) complexes described here provide a textbook example of this electronic/geometric interplay.

Results and Discussion

Synthesis and Electrochemical Properties. The new complexes, Cp_2Mo(dmit), Cp_2Mo(dmio), and Cp_2Mo(dddt), were prepared by the conventional metathetical reaction of Cp_2MoCl_2 with the dithiolene disodium salt, generated from the corresponding bis(thioester) or dithiocarbonate with NaOMe. As already observed by Green[17] and Klapötke,[22] Cp_2MoCl_2 appears more reluctant to reaction with thiolates than the analogous Cp_2TiCl_2 which lacks two electrons. Thus, reactions had to be conducted in refluxing THF or $CHCl_3$ for longer periods of time, while the formation of Cp_2Ti(dmit) or Cp_2Ti(dddt), for example, was accomplished at room temperature in a few hours[14] (Scheme 1).

Cp_2Mo(dmit) and Cp_2Mo(dmio) derivatives were found to be air stable. Cp_2Mo(dddt) is readily oxidized in solutions exposed to air but is stable in the solid state. Each complex but Cp_2Mo(dddt), which reduces irreversibly, exhibits one reversible reduction wave at −2.0 V *vs* Ag/Ag^+ and two reversible oxidation waves (Figure 1). This is in contrast with the behavior of thiolate complexes reported by Kotz et al.[23] such as $Cp_2Mo(SR)_2$, R = Me, Ph in which the first oxidation was

(14) (a) Bolinger, C. M.; Rauchfuss, T. B. *Inorg. Chem.* **1982**, *21*, 3947. (b) Yang, X.; Rauchfuss, T. B.; Wilson, S. R. *J. Am. Chem. Soc.* **1989**, *111*, 3465. (c) Guyon, F.; Lenoir, C.; Fourmigué, M.; Larsen, J.; Amaudrut, J. *Bull. Soc. Chim. Fr.* **1994**, *131*, 217.
(15) (a) Viard, B.; Amaudrut, J.; Sala-Pala, J.; Fakhr, A.; Mugnier, Y.; Moise, C. *J. Organomet. Chem.* **1985**, *292*, 403. (b) Guyon, F.; Amaudrut, J.; Mercier, M.-F.; Shimizu, K. *J. Organomet. Chem.* **1994**, *465*, 187.
(16) (a) Green, M. L. H.; Lindsell, W. E. *J. Chem. Soc. A* **1967**, 1455. (b) Kutoglu, A.; Köpf, H. *J. Organomet. Chem.* **1970**, *25*, 455.
(17) Green, M. L. H.; Heuer, W. B.; Saunders, G. C. *J. Chem. Soc., Dalton Trans.* **1990**, 3789.
(18) Lauher, J. W.; Hoffmann, R. *J. Am. Chem. Soc.* **1976**, *98*, 1729.
(19) (a) Stephan, D. W. *Inorg. Chem.* **1992**, *31*, 4218. (b) Guyon, F.; Fourmigué, M.; Amaudrut, J. To be submitted for publication.
(20) (a) Huber, W.; Müllen, K. *Acc. Chem. Res.* **1986**, *19*, 300. (b) Jørgensen, M.; Lerstrup, K.; Frederiksen, P.; Bjørnholm, T.; Sommer-Larsen, P.; Schaumburg, K.; Brunfeldt, K.; Bechgaard, K. *J. Org. Chem.* **1993**, *58*, 2785. (c) Boubekeur, K.; Lenoir, C.; Batail, P.; Carlier, R.; Tallec, A.; Le Paillard, M.-P.; Lorcy, D.; Robert, A. *Angew. Chem., Int. Ed. Engl.* **1994**, *33*, 1379.
(21) See, for example: (a) Darensbourg, M. Y.; Silva, R.; Reibenspies, J.; Prout, C. K. *Organometallics* **1989**, *8*, 1315. (b) Gowik, P.; Klapötke, T.; Pickardt, J. *Organometallics* **1989**, *8*, 2953.
(22) (a) Gowik, P. K.; Klapötke, T. M.; White, P. *Chem. Ber.* **1989**, *122*, 1649. (b) Gowik, P. K.; Klapötke, T. M. *Inorg. Chim. Acta* **1990**, *169*, 1.
(23) Kotz, J. C.; Vining, W.; Coco, W.; Rosen, R.; Dias, A. R.; Garcia, M. H. *Organometallics* **1983**, *2*, 68.
(24) Knox, J. R.; Prout, C. K. *J. Chem. Soc., Chem. Commun.* **1967**, 1277.
(25) Pilato, R. S.; Eriksen, K. E.; Greaney, M. A.; Stiefel, E. I.; Goswami, S.; Kilpatrick, L.; Spiro, T. G.; Taylor, E. C.; Rheingold, A. L. *J. Am. Chem. Soc.* **1991**, *113*, 9372.

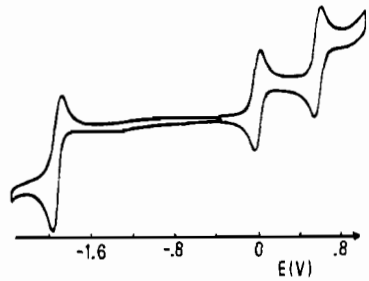

Figure 1. Cyclic voltamogram of $Cp_2Mo(dmit)$. Scan rate 100 mV s^{-1}

Table 1. Cyclic Voltammetry Data (V *vs* $Ag/AgClO_4$ (0.1 M))[a]

compound	E_p^{red}	$E_{1/2}^0$	$E_{1/2}^1$	$E_{1/2}^2$
Cp_2MoCl_2[b]	−1.82		0.135	0.72
$Cp_2Mo(dmit)$		−1.99	−0.01 (60)	0.575 (60)
$Cp_2Mo(dmio)$		−2.05	−0.075 (70)	0.555 (80)
$Cp_2Mo(dddt)$	<−2.1		−0.34 (60)	0.26 (65)
$Cp_2Mo[S_2C_2(SR)_2]$[c]			−0.295 (60)	0.19 (60)

[a] In parenthesis are given the separation between the anodic and cathodic peak potentials (mV). [b] From ref 23. [c] From ref 17, $(SR)_2 = -S(CH_2CH_2O)_3CH_2CH_2S-$.

described as reversible while the second oxidation led to decomposition *via* an EEC process. Note, however, that despite this electrochemical irreversible behavior, Mo^{VI} species of formula $[Cp_2Mo(SR)_2][AsF_6]_2$ have been recently isolated[22] either by direct oxidation of $Cp_2Mo(SR)_2$ with AsF_5 or by reaction of thiols with $[Cp_2Mo^{VI}Cl_2][AsF_6]_2$. The dithiolene nature of the ligand thus appears to strongly stabilize the oxidized Mo^V and Mo^{VI} species. Note also that, as expected from the redox potentials of various homoleptic dithiolene complexes, oxidations are easiest with the $dddt^{2-}$ ligand with the ordering $dddt^{2-} > dmio^{2-} \geq dmit^{2-}$ (Table 1). The substitution of dithiolene ligands for the chlorine atoms lowers dramatically the oxidation potentials of the complexes, affording $Mo(d^1)$ 17 e^- and $Mo(d^0)$ 16 e^- species probably now amenable to isolation and manipulation in the air.

Therefore, oxidation of these novel electron donors was investigated with the organic acceptor TCNQ. Two black crystalline phases were isolated from the reaction with $Cp_2Mo(dddt)$: very thin needles, of 2:3 stoichiometry, which were too small for an X-ray structural analysis, and platelets, whose 1:1 stoichiometry was ascertained by the structure determination (see below). On the contrary, $Cp_2Mo(dmit)$ or $Cp_2Mo(dmio)$ did not not react with TCNQ, probably because their oxidation potential is too high, when compared to the reduction potential of TCNQ.

Structural Properties *vs* Electron Count: An EH Rationale. Single crystal X-ray structure determinations were conducted on the neutral d^2 Mo^{IV} compound $Cp_2Mo(dddt)$ and its 1:1 TCNQ salt in order to compare the geometry around the metal atom in the 18- and 17-electron complexes. $Cp_2Mo(dddt)$ crystallizes in the orthorhombic system, space group $Pna2_1$, with $a = 16.608(3)$ Å, $b = 11.568(2)$ Å, and $c = 7.724(1)$ Å; the molecule is located in general position in the unit cell (Figure 2). Final positional and equivalent thermal parameters are given in Table 2; important geometrical features, in Table 3. As seen from Table 3, $Cp_2Mo(dddt)$ is similar to other crystallographically characterized dithiolene complexes of molybdocene. However, the folding of the ligand plane respective to the S−Mo−S plane, usually ranging from 0 to 9°, increases up to 13(1)° in $Cp_2Mo(dddt)$.

The 1:1 salt $[Cp_2Mo(dddt)][TCNQ]$ crystallizes in the triclinic system, space group $P\bar{1}$ with $a = 9.597(1)$ Å, $b = 10.543(4)$ Å, $c = 12.460(3)$ Å, $\alpha = 84.41(2)°$, $\beta = 80.94(2)°$, and $\gamma = 89.41(2)°$. Both molecules are located in general position in the unit cell (Figure 3). Final positional and equivalent thermal parameters are given in Table 4, important geometrical features, in Table 3. In the following, we concentrate on $Cp_2Mo(dddt)^{\bullet+}$ geometry and will discuss in the third part of this paper the geometry of $TCNQ^{\bullet-}$ as well as the solid-state arrangement and electronic properties of $[Cp_2Mo(dddt)][TCNQ]$.

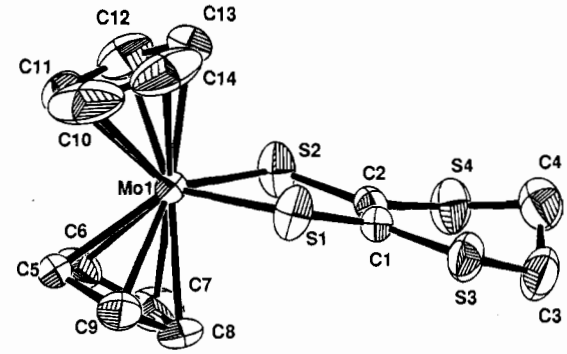

Figure 2. ORTEP drawing and numbering scheme for $Cp_2Mo(dddt)$. Thermal ellipsoids are drawn at the 50% probability level.

Table 2. Atomic Positional and Isotropic Thermal Parameters for $Cp_2Mo(dddt)$

	x/a	*y/b*	*z/c*	B_{eq}[a] (Å^2)
Mo	0.64811(3)	0.61138(4)	0.207	2.550(8)
S(1)	0.5065(1)	0.6626(2)	0.2364(3)	4.02(4)
S(2)	0.6649(1)	0.7832(2)	0.3866(3)	4.05(4)
S(3)	0.4007(1)	0.7973(2)	0.4527(3)	4.35(4)
S(4)	0.5721(1)	0.9330(2)	0.6119(3)	4.67(5)
C(1)	0.5019(4)	0.7673(5)	0.3986(9)	2.9(1)
C(2)	0.5672(4)	0.8190(5)	0.4604(9)	2.9(1)
C(3)	0.4100(6)	0.8949(8)	0.632(1)	5.4(2)
C(4)	0.4721(6)	0.9880(8)	0.603(1)	5.2(2)
C(5)	0.6932(4)	0.4266(6)	0.235(1)	4.0(2)
C(6)	0.7389(5)	0.4934(6)	0.347(1)	4.4(2)
C(7)	0.6881(7)	0.5363(8)	0.478(1)	5.7(2)
C(8)	0.6099(6)	0.4976(7)	0.438(1)	5.9(2)
C(9)	0.6115(5)	0.4301(7)	0.290(1)	4.9(2)
C(10)	0.6595(9)	0.563(1)	−0.087(1)	9.3(4)
C(11)	0.7351(6)	0.5908(8)	−0.025(1)	6.7(2)
C(12)	0.7358(5)	0.7027(8)	0.021(1)	5.6(2)
C(13)	0.6604(6)	0.7456(7)	−0.014(1)	5.8(2)
C(14)	0.6138(6)	0.661(1)	−0.080(1)	7.2(3)

[a] $B_{eq} = {}^4/_3[a^2B(1,1) + b^2B(2,2) + c^2B(3,3) + ab\cos\gamma\, B(1,2) + ac\cos\beta\, B(1,3) + bc\cos\alpha\, B(2,3)]$.

The most striking feature in $Cp_2Mo(dddt)^{\bullet+}$ is the angle between the ligand plane and the S−Mo−S plane which amounts now to 32.1(1)°. The folding angle has thus increased by nearly 20° upon removal of one electron from the HOMO. At the same time, the dithiolene fragment adopts a more dithioketonic structure, as shown by the shortening of the C−S bonds and the related lenghtening of the C=C bond. This behavior tends to indicate that the oxidation not only involves the d^2 Mo atom but also the dithiolene ligand. A similar delocalization of the spin has been deduced from EPR in the solution of paramagnetic d^1 Cp_2Nb(dithiophosphate) complexes.[26] In order to get a deeper insight into the electronic structure of those componds, EH calculations[27] were conducted on $Cp_2Mo(dddt)$ for different hypothetical geometries. The interaction diagram between the Cp_2Mo and the dithiolene fragments in the ideal C_{2v} conformation (no ligand folding) is shown in Figure 4. The slightly antibonding HOMO is mainly

(26) Sanchez, C.; Vivien, D.; Livage, J.; Sala-Pala, J.; Viard, B.; Guerchais, J. *J. Chem. Soc., Dalton Trans.* **1981**, 4.
(27) Albright, T. A.; Burdett, J. K.; Whangbo, M.-H. In *Orbital Interactions in Chemistry*; Wiley: New York, 1985; Chapter 20, pp 381−401.

Table 3. Geometrical Features of Cp_2Mo(dithiolene) Complexes

dithiolene	Mo−S (Å)	C−S (Å)	C−C (Å)	S−Mo−S (deg)	folding angle, θ (deg)	ref
$S_2C_6H_3Me$	2.43(3)	1.78(1)	1.35(3)	82.(2)	2.6	24
$S_2C_6H_4$	2.437(3)			81.9(5)	9	16b
S_2C_2RR'[a]	2.437(2)	1.762(8)	1.338(12)	82.2(2)	0	25
dddt	2.435(2)	1.76(1)	1.33(1)	81.90(7)	13.3(5)	this work
dddt in the $Cp_2Mo(dddt)^{n+}$	2.425(7)	1.725(7)	1.373(1)	80.38(2)	32.1(1)	this work

[a] R, 2-quinoxalinyl; R', acetyl.

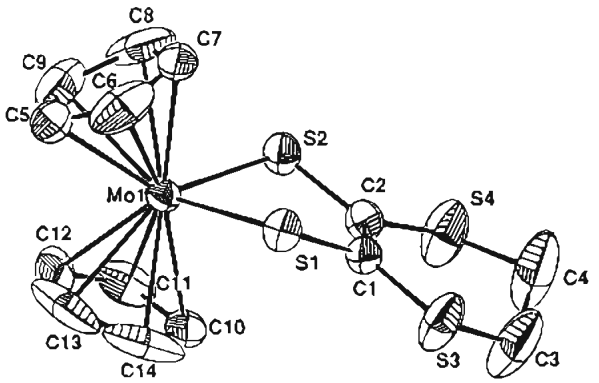

Figure 3. ORTEP drawing and numbering scheme for $Cp_2Mo(dddt)^{n+}$ in $[Cp_2Mo(dddt)][TCNQ]$. Thermal ellipsoids are drawn at the 50% probability level.

Table 4. Positional and Isotropic Displacement Parameters for $[Cp_2Mo(dddt)][TCNQ]$

	x/a	*y/b*	*z/c*	10^2U_{eq}[a]
Mo	0.22919(4)	1.00169(4)	0.20034(3)	3.36(1)
S(1)	0.3899(1)	0.8268(1)	0.1650(1)	3.75(4)
S(2)	0.1866(1)	0.9651(1)	0.01870(9)	3.93(4)
S(3)	0.3648(2)	0.5863(1)	0.0794(1)	6.61(6)
S(4)	0.1461(2)	0.7395(2)	−0.0872(2)	7.39(7)
C(1)	0.3117(5)	0.7444(4)	0.0768(4)	3.6(1)
C(2)	0.2245(5)	0.8055(5)	0.0117(4)	3.8(2)
C(3)	0.266(1)	0.5198(7)	−0.0116(7)	10.2(4)
C(4)	0.246(1)	0.5974(8)	−0.1086(7)	11.2(5)
C(5)	0.3222(7)	1.1665(6)	0.2774(5)	6.0(2)
C(6)	0.4301(6)	1.1048(6)	0.2250(8)	7.7(3)
C(7)	0.4231(8)	1.1188(7)	0.1176(7)	8.1(3)
C(8)	0.309(1)	1.1909(7)	0.1021(6)	9.8(4)
C(9)	0.2440(7)	1.2211(6)	0.2048(7)	7.1(3)
C(10)	0.0569(6)	0.8477(5)	0.2526(5)	5.4(2)
C(11)	−0.0100(5)	0.9654(7)	0.2476(5)	5.9(2)
C(12)	0.0298(8)	1.0323(7)	0.3249(7)	8.2(3)
C(13)	0.118(1)	0.961(1)	0.3782(5)	10.4(4)
C(14)	0.1345(6)	0.8481(9)	0.3380(7)	8.8(3)
N(1)	0.0012(5)	0.5205(6)	0.7386(4)	6.3(2)
N(2)	0.0849(5)	0.2663(5)	0.4753(4)	5.4(2)
N(3)	0.7609(5)	0.7142(4)	0.1676(4)	4.9(1)
N(4)	0.6858(5)	0.9721(5)	0.4245(4)	6.2(2)
C(15)	0.2712(4)	0.5375(4)	0.5114(4)	3.2(1)
C(16)	0.3089(5)	0.6521(4)	0.5524(4)	3.5(1)
C(17)	0.4212(5)	0.7240(4)	0.5016(4)	3.5(1)
C(18)	0.5073(4)	0.6889(4)	0.4059(4)	3.1(1)
C(19)	0.4682(4)	0.5746(4)	0.3646(3)	3.3(1)
C(20)	0.3569(4)	0.5034(4)	0.4146(4)	3.3(1)
C(21)	0.1556(5)	0.4607(5)	0.5635(4)	3.5(1)
C(22)	0.0691(5)	0.4941(5)	0.6606(4)	4.3(2)
C(23)	0.1151(4)	0.3527(5)	0.5167(4)	3.8(1)
C(24)	0.6248(4)	0.7640(4)	0.3515(4)	3.2(1)
C(25)	0.6594(5)	0.8787(5)	0.3918(4)	4.1(2)
C(26)	0.7011(4)	0.7354(4)	0.2499(4)	3.5(1)

[a] $U_{eq} = {}^1/_3\sum_i\sum_j U_{ij}\, a_i^* a_j^* \mathbf{a}_i\mathbf{a}_j$.

of metal character (an a_1 combination of d_{z^2} and $d_{x^2-y^2}$) while HOMO-1 consists almost exclusively of the π-orbital of the dithiolene ligand with a weak interaction with metal orbitals of d_{xz} character. Upon oxidation, the system stabilizes by mixing the two fragment orbitals (a_1 and π), an interaction which, for

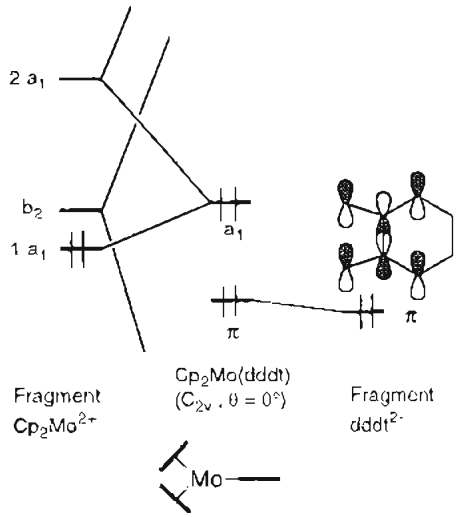

Figure 4. Interaction diagram for $Cp_2Mo(dddt)$ in the unfolded (C_{2v}) geometry.

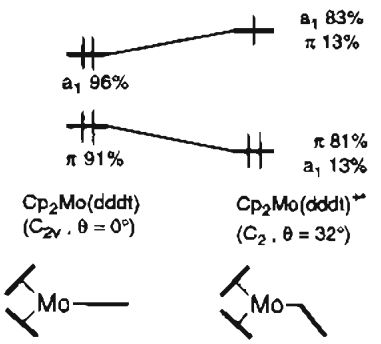

Figure 5. Changes in the frontier orbital HOMO and HOMO-1 of $Cp_2Mo(dddt)$ upon oxidation and concomitant ligand bending from 0 to 32°.

symmetry reasons, is only possible when the ligand folds (Figure 5). The contribution of the dithiolene π fragment orbital to the SOMO becomes then nonnegligible, explaining the observed shortening of the C−S bond (of antibonding character in the π fragment orbital) and lengthening of the central C−C bond (of bonding character) of the dithiolene. To which extent the ligand could fold can be inferred from a plot of the energy difference $\Delta E = E_\theta - E_{\theta=0}$ *vs* the folding angle θ for different electron counts (Figure 6). For the neutral d^2 $Cp_2Mo(dddt)$, a flat minimum is observed at 0° and an unfolded structure is then expected, while, for the oxidized d^1 complex, one expects the ligand to fold, however, with a low energy gain and in a large angle range. For the hypothetical d^0 $Cp_2Mo(dddt)^{2+}$, a clear minimum is observed and hence a folded structure can be predicted, as already observed in the analogous d^0 Cp_2Ti(dithiolene) complexes.[14] Certainly there is a tendency to fold when the system is oxidized, in qualitative agreement with our findings.

Structural Analysis of $[Cp_2Mo(dddt)][TCNQ]$. In the structure of $[Cp_2Mo(dddt)][TCNQ]$, $TCNQ^{\bullet-}$ are associated into centrosymmetrical dimers located at the center of the unit cell

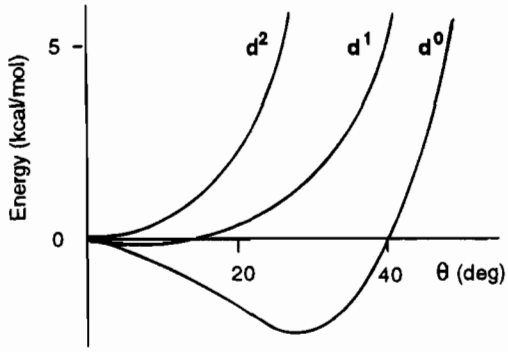

Figure 6. Total energy change for the bending (θ) of the ligand for $Cp_2Mo(dddt)$ in the neutral (d^2), cationic (d^1), or dicationic (d^0) states.

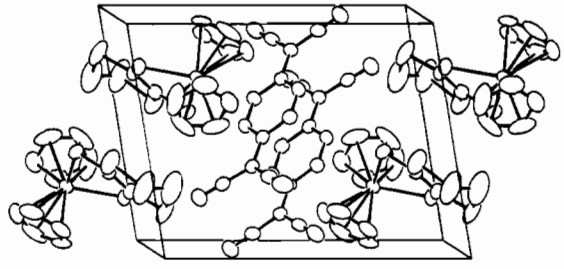

Figure 7. ORTEP view of the unit cell of [$Cp_2Mo(dddt)$][TCNQ]. The *c* axis runs horizontally and the *a* axis vertically. The *b* axis is approximately normal to the figure.

with a ring-over-ring overlap and a short-axis slip of 1.11 Å (Figure 7). Similar geometrical characteristics have already been encountered in a variety of dimeric TCNQ salts such as Rb(TCNQ),[28] $Cs_2(TCNQ)_3$,[29] (A-18-crown-6)(TCNQ),[30] A = Na^+, K^+, Rb^+, Tl^+, or the so-called "dimeric" phase of ($(Cp^*)_2Fe$)(TCNQ).[31] In those compounds the overlap within the dimer is characterized by a negligible molecular long-axis slip (ring-over-ring overlap) but a significant short-axis slip, from 0.33 to 0.7 Å in the crown-ether derivatives[30] up to 1.0 Å in ($(Cp^*)_2$Fe)(TCNQ).[31] These peculiarities have been associated with the occurrence of *isolated* dimers,[30] contrary to the situation encountered in most TCNQ salts where the acceptor molecules exhibit a strong tendency to stack in the solid state. The intradimer plane-to-plane distance, 3.20(1) Å, lies in the order of magnitude of the distances observed in the above-mentioned $TCNQ_2^{2-}$ moieties. Also the intramolecular distances within an individual $TCNQ^{\bullet-}$ point toward a fully reduced anion radical. Based on the large number of reported salts, three different correlations between the charge of the molecule and the bond lengths have been reported.[32] Applying those three correlations to the TCNQ bond lengths in [$Cp_2Mo(dddt)$]-[TCNQ], averaged in D_{2h} symmetry, gives calculated charges of −0.99, −0.99, and −0.97, thus confirming the total charge-transfer character of the salt, as anticipated from the electrochemical data. Thus, the TCNQ dimers can be tentatively described as isolated fully reduced dianionic $(TCNQ_2)^{2-}$ moieties.

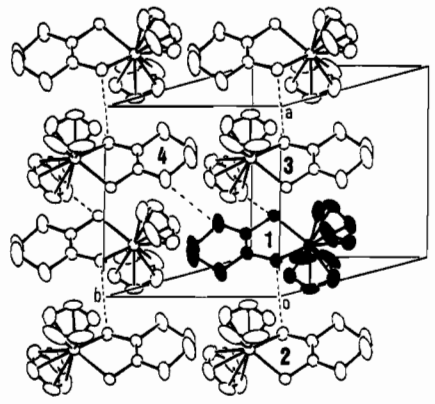

Figure 8. View of the *ab* plane in [$Cp_2Mo(dddt)$][TCNQ]. The main intermolecular interactions are shown with dash lines (see text).

In the solid, from an analysis of the shortest intermolecular contacts, we can identify layers of $Cp_2Mo(dddt)^{\bullet+}$ cation radicals parallel to the *ab* plane, separated from each other by the $(TCNQ_2)^{2-}$ dimers (Figure 8). Within the layers, the intermolecular Mo−Mo distances amount to 6.61 and 7.15 Å along the *a* axis, while they exceed 12 Å in the *b* direction. Thus, this salt could be described as slightly dimerized chains of $Cp_2Mo(dddt)^{\bullet+}$ separated by the $(TCNQ_2)^{2-}$ dimers. Note, however, that the intermolecular Mo−Mo distances may not be the only parameter for accounting for the electronic structure of the material (see below) since a part of the spin density is actually delocalized on the dithiolene ligand.

Antiferromagnetic Interactions in [$Cp_2Mo(dddt)^{\bullet+}$]-[$TCNQ^{\bullet-}$]. EPR experiments performed on oriented single crystals show a single anisotropic signal with a Lorentzian shape at all temperatures. An extremum of *g* values was found with the *a* axis of the crystal parallel to the external magnetic field. In the plane perpendicular to *a*, the two other extrema were observed at angles between the plane of the platelet and the external magnetic field of 45° and 135°. The eigenvalues for the **g**-tensor, as deduced from these experiments, are the following: $g_{min} = 1.9887$, $g_{int} = 2.0096$, $g_{max} = 2.0192$, with g_{max} along the *a* axis and g_{int} and g_{min} in a plane perpendicular—in first approximation—to the *a* axis. The anisotropy of the line width is weak (26−29 G) with the smallest value found for an orientation close to that of g_{int}. The *g* factor was found to be temperature independent.

The SQUID magnetic susceptibility was measured from room temperature down to 4.2 K under a magnetic field of 3 kG (Figure 9). Data were corrected for diamagnetic and sample holder contributions. The SQUID susceptibilty was found to follow a Curie−Weiss behavior in the high-temperature regime with $\Theta = -42 \pm 2$ K. A maximum was then reached at $T(\chi_{max}) = 32$ K with $\chi_{max}/\chi_{rt} = 4.5$.

The structural description of the salt suggested a slightly dimerized one-dimensional chain of spin $^1/_2$ $Cp_2Mo(dddt)^{\bullet+}$ cation radicals, separated by strongly dimerized $(TCNQ_2)^{2-}$ pairs. From the literature data[30,31] we can expect the TCNQ dimers either to be EPR silent or to possess a weak susceptibility derived from a thermally activated triplet state. This is confirmed by the comparison of the measured effective moment, $\mu_{eff} = [3\,\chi_\pi k_B(T - \Theta)/N]^{1/2} = 1.77\,\mu_B$/Mo, a value very close to the calculated one for one spin $^1/_2$ only[3] (1.73 μ_B). Thus we can consider our magnetic system to be almost exclusively formed of the chains of $Cp_2Mo(dddt)^{\bullet+}$ surrounded by magneti-

(28) Hoekstra, A.; Spoelder, T.; Vos, A. *Acta Crystallogr. B* **1972**, *28B*, 14.
(29) Fritchie, C. J., Jr.; Arthur, P., Jr. *Acta Crystallogr.* **1966**, *21*, 139.
(30) (a) Grossel, M. C.; Evans, F. A.; Hriljac, J. A.; Morton, J. R.; LePage, Y.; Preston, K. F.; Sutcliffe, L. H.; Williams, A. J. *J. Chem. Soc., Chem. Commun.* **1990**, 439. (b) Grossel, M. C.; Evans, F. A.; Hriljac, J. A.; Prout, K.; Weston, S. C. *J. Chem. Soc., Chem. Commun.* **1990**, 1494. (c) Grossel, M. C.; Weston, S. C. *J. Chem. Soc., Chem. Commun.* **1992**, 1510.
(31) (a) Reis, A. H., Jr.; Preston, L. D.; Williams, J. M.; Peterson, S. W.; Candela, G. A.; Schwartzendruber, L. J.; Miller, J. S. *J. Am. Chem. Soc.* **1979**, *101*, 2756. (b) Miller, J. S.; Zhang, J. H.; Reiff, W. M.; Dixon, D. A.; Preston, L. D.; Reis, A. H., Jr.; Gebert, E.; Extine, M.; Troup, J.; Epstein, A. J.; Ward, M. D. *J. Phys. Chem.* **1987**, *91*, 4344.
(32) . (a) Flandrois, S.; Chasseau, D. *Acta Crystallogr.* **1977**, *33B*, 2744. (b) Kistenmacher, T. J.; Emge, T. J.; Bloch, A. N.; Cowan, D. O. *Acta Crystallogr.* **1982**, *38B*, 1193. (c) Umland, T. C.; Allie, S.; Kulhman, T.; Coppens, P. *J. Phys. Chem.* **1988**, *92*, 6456.

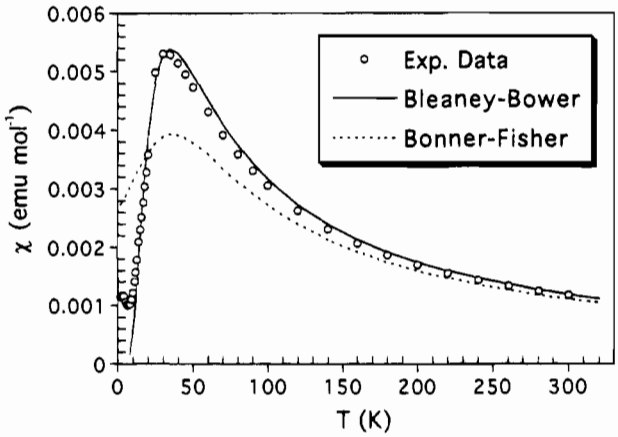

Figure 9. Temperature dependence of the SQUID susceptibility for $[Cp_2Mo(dddt)][TCNQ]$.

cally silent $(TCNQ)_2^{2-}$. A very similar situation was probably encountered in the dimeric phase of $((Cp^*)_2Fe)(TCNQ)$ where magnetism originating only from the $((Cp^*)_2Fe)^{\bullet+}$ cations was observed.[31]

The magnetic behavior of our system—Curie–Weiss in the high temperature regime with $\Theta = -42$ K, followed by a rounded susceptibility maximum—is characteristic of a one-dimensional system of antiferromagnetically interacting spins. Two limiting cases have been investigated in detail: the regular spin chain by Bonner and Fischer[33-35] and the strongly dimerized system by Bleaney and Bower. Intermediate situations have also been studied.[35-38] If we define J as the exchange integral coupling a spin with its nearest right neighbor and αJ as the exchange integral coupling a spin with its nearest left neighbor ($0 \leq \alpha \leq 1$), the Bonner–Fisher situation corresponds to $\alpha = 1$, while $\alpha = 0$ leads to the Bleaney–Bower system. It has been shown[35,38] that the temperature of maximum susceptibility, $T(\chi_{max})$, is nearly independant of α and can be expressed as $kT(\chi_{max}) = (1.27 \pm 0.2)|J|$. Thus, we can deduce from our data an approximate J/k value of -25 to -26 K.

The experimental data were fitted very satisfactorily (for $10 \leq T \leq 300$ K, $R = 0.985$) with the Bleaney–Bower equation which reads $\chi = Ng^2\mu_B{}^2/kT(3 + \exp^{-2J/kT})^{-1}$ with $J/k = -28$ K. A superimposable curve was also obtained within the alternating chain model[35] with $J/k = -25.5$ K and $\alpha = 0.22$. Both fits lead to the conclusion of the presence of strongly dimerized chains of spins.

From the structural determination of $[Cp_2Mo(dddt)^{\bullet+}][TCNQ^{\bullet-}]$, we know that the Mo–Mo distances within a chain are not uniform (6.61 and 7.15 Å). However, since these distances are too large for supporting the possibility of a direct Mo–Mo interaction, intermolecular interactions through ligand–ligand (Cp, dddt) overlaps are needed. Those overlaps may not be negligible since we know the spin to be partially delocalized on the $dddt^{2-}$ ligand in the SOMO.

The strength of the intermolecular interactions can be quantified by calculating the associated $\beta_{HOMO-HOMO}$ interaction energies. The β_{ij} interaction energy between two orbitals i and j is defined as

$$\beta_{ij} = \sum_{\mu}\sum_{\nu} c_{\mu i}c_{\nu j}\langle\chi_\mu|H^{eff}|\chi_\nu\rangle \quad (1)$$

where $c_{\mu i}$ is the coefficient of atomic orbital χ_μ in the molecular orbital Ψ_i.

$$\Psi_i = \sum_{\mu} c_{\mu i}\chi_\mu \quad (2)$$

These interaction energies have proved to be very useful in discussing the electronic structure of many organic charge-transfer salts.[39] The strongest calculated β values, 0.042 and 0.019 eV, are found along the a axis for interactions between molecules 1 and 2 and 1 and 3, respectively (Figure 8). Interaction 1–2 relies mainly on a $S(2)_1$–$S(2)_2$ (3.739 Å) overlap, while interaction 1–3 is due to a $S(1)_1$–$C(7)_3$ (3.684 Å) short contact. The corresponding transfer energies t_{ij} between the interacting HOMOs amount to 0.027 and 0.012 eV, respectively.

A much weaker interaction (0.007 eV) accounts for an $S(3)_1$–$S(3)_4$ (3.598 Å) interchain overlap. Albeit the latter S–S distance is rather short, the HOMO coefficients of the $Cp_2Mo(dddt)$ on the outer sulfur atoms of the dithiine ring [S(3) and S(4)] are very small, thus explaining this weak β_{1-4} value. Note that since all those interaction energies remain small, the β_{ij} and t_{ij} absolute values are expected to be very sensitive to small geometrical changes and hence definitive conclusions from the numerical values deduced from the room temperature crystal structure should be taken with care for evaluating the interaction energies in the low temperature regime.

In a Hubbard model, with U describing the on-site electronic repulsion and t the resonance integral, the exchange integral J between two adjacent sites writes as t^2/U.[1b] Thus, we expect the ratio $(t_{1-3}/t_{1-2})^2$ to behave approximately as $J_{1-3}/J_{1-2} = \alpha$. The calculated value of 0.25 for $(t_{1-3}/t_{1-2})^2$ compares indeed favorably with the α value deduced from the numerical fit of χ.

Antiferromagnetic interactions have been recently reported in a series of d^1 molybdenum compounds[40] of general formula $[Mo(\eta\text{-}C_7H_7)(MeCN)X_2]$, X = Br, I, which adopt uniform linear structures. The weaker ($\Theta = -4 \pm 1$ K, $T(\chi_{max}) = 14 \pm 2$ K, $J_{//} = -9 \pm 1$ K) antiferromagnetic interactions observed in those compounds illustrate the ability of the dithiolene complexes to interact strongly in the solid state.

Despite the presence of antiferromagnetic interactions, the absence of any transition to an ordered three-dimensional antiferromagnetic ground state may be related to the layered structure adopted by the paramagnetic cations in $[Cp_2Mo(dddt)][TCNQ]$.

Conclusion

Cp_2Mo(dithiolene) complexes appear to be very promising candidates for the elaboration of novel materials with interesting electronic properties. The reversible redox character is confirmed by the isolation and crystal structure resolution of the the 17-electron oxidized d^1 $Cp_2Mo(dddt)^{\bullet+}$, whose folded geometry can be rationalized by the extended Hückel calculations. The presence of strong antiferromagnetic interactions in a TCNQ salt of $Cp_2Mo(dddt)$ demonstrates the capabilities of

(33) Bonner, J. C., Fisher, M. E. *Phys. Rev. A* **1964**, *135*, 640.
(34) See the note given under ref 60 in: Torrance, J. B.; Tomkiewicz, Y.; Silverman, B. D. *Phys. Rev. B* **1977**, *15*, 4738.
(35) (a) Hall, J. W. Ph.D. Dissertation, University of North Carolina, Chapel Hill, NC, 1980. (b) Hatfield, W. E. *J. Appl. Phys.* **1981**, *52*, 1985.
(36) Bulaevski, L. N. *Sov. Phys.—Solid State* **1969**, *11*, 921.
(37) Duffy, W., Jr.; Barr, K. P. *Phys. Rev.* **1968**, *165*, 647.
(38) Bonner, J. C.; Blöte, H. W. J.; Bray, J. W.; Jacobs, I. S. *J. Appl. Phys.* **1979**, *50*, 1810.
(39) (a) Williams, J. M.; Wang, H. H.; Emge, T.; Geiser, U.; Beno, M. A.; Leung, P. C. W.; Carlson, K. D.; Schulz, A. J.; Whangbo, M.-H. In *Progress in Inorganic Chemistry*, Lippard, S. J., Ed.; Interscience: New York, 1987; Vol. 35, pp 51–218. (b) Pénicaud, A.; Boubekeur, K.; Batail, P.; Canadell, E.; Auban-Senzier, P.; Jérome, D. *J. Am. Chem. Soc.* **1993**, *115*, 4101.
(40) Green, M. L. H.; Harrison, A.; Mountford, P.; Ng, D. K. P. *J. Chem. Soc., Dalton Trans.* **1993**, 2215.

those molecules to interact with each other in the solid state. Further work will concentrate on the elaboration of other materials with different dithiolene ligands and smaller anionic counterparts as well as on the preparation of bimetallic compounds.

Experimental Section

General Data. Solvents were dried and distilled just prior to use and the air-sensitive dithiolenes manipulated under argon using standard vacuum-line techniques. Cp_2MoCl_2 was obtained from Strem Chemical or prepared following ref 41. NMR spectra were recorded in $CDCl_3$ with TMS as the internal standard, on a 200-MHz Brucker spectrometer. Elemental analysis was performed at the Institut de Chimie des Substances Naturelles, CNRS, Gif/Yvette, France.

$Cp_2Mo(dmit)$, Bis(η^5-cyclopentadienyl)(2-thioxo-1,3-dithiole-4,5-dithiolato)molybdenum(IV). A suspension of Cp_2MoCl_2 (1 equiv) and Na_2dmit[42] (1.1 equiv) in $CHCl_3$ was refluxed for 2 days. The violet solution was filtered and concentrated and the residue chromatographed on SiO_2 (el. CH_2Cl_2), yield 55%, mp >250 °C (from CH_2Cl_2). IR (KBr): 3100 f (Cp), 1442 F (C=C), 1412 m, 1360 m, 1049 F (C=S), 1032 F (C=S), 1025 F (Cp), 1010 m (Cp), 992 m, 886 f, 830 F (Cp), 814 F (Cp), 521 f, 460 f cm^{-1}. ^1H NMR ($CDCl_3$, TMS): δ_H 5.40 (s, Cp).

$Cp_2Mo(dmio)$, Bis(η^5-cyclopentadienyl)(2-oxo-1,3-dithiole-4,5-dithiolato) molybdenum(IV). It was prepared as above, from Na_2-dmio, obtained by reaction of thiapendione[43] with MeONa (2 equiv) and precipitation with Et_2O, yield 55%, mp >250 °C (from CH_2Cl_2). IR (KBr): 3100 m (Cp), 1656 F (C=O), 1598 F, 1482 m, 1431 m, 1417 m, 1017 m (Cp), 1000 m, 902 m, 885 m, 833 F (Cp), 815 F (Cp), 751 m, 468 m cm^{-1}. ^1H NMR ($CDCl_3$, TMS): δ_H 5.37 (s, Cp).

$Cp_2Mo(dddt)$, Bis(η^5-cyclopentadienyl)(5,6-dihydro-1,4-dithiine-2,3-dithiolato)molybdenum(IV). As above from Na_2dddt[44] and Cp_2MoCl_2, one obtains a grey-blue powder, recrystallized by slow addition of AcOEt in a concentrated CH_2Cl_2 solution, yield 50%, mp > 250 °C (from CH_2Cl_2/AcOEt). IR (KBr) 3100 m (Cp), 2953 f (C—H), 2909 f (C—H), 1431 m, 1416 m, 1283 m, 1016 f (Cp), 1000 m (Cp), 919 f (C—S), 831 F (Cp), 813 F (Cp) cm^{-1}. ^1H NMR ($CDCl_3$, TMS): δ_H 5.29 (s, 10H, Cp), 3.13 (s, 4H, CH_2).

Satisfactory elemental analyses were obtained for the three compounds.

[$Cp_2Mo(dddt)$][TCNQ]. Warm solutions of $Cp_2Mo(dddt)$ (41 mg, 0.1 mmol) in CH_3CN (125 mL) and TCNQ (21 mg, 0.1 mmol) in CH_3CN (10 mL) were mixed and cooled slowly. Large crystals of the title compound (12 mg) precipitate from the cooled solution together with bundles of very thin needles which could be removed by hand.

The latter needlelike crystals were found to be too small for X-ray investigations. Elemental analysis points toward a 2:3 stoichiometry, i.e., $[Cp_2Mo(dddt)]_2[TCNQ]_3$. Calcd for $C_{64}H_{40}S_8Mo_2N_{12}$ (Found): C, 53.93 (53.73); H, 2.83 (2.92); N, 11.79 (11.75).

Electrochemical Measurements. Cyclic voltammetry experiments were performed with a SOTELEM P/T potentiostat coupled with a PAR 175 universal programmer. Acetonitrile dried on molecular sieves with 0.1 M n-$Bu_4N^+PF_6^-$ was used as electrolyte. A three compartment cell was used, fitted with a 2-mm-diameter platinum working electrode, a platinum counter electrode, and an $Ag/AgClO_4$ (0.1 M) reference electrode.

Crystal Structure Determinations. The unit-cell parameters were determined from a least-squares refinement of the angular settings of 25 well centered reflections. Crystallographic data and additional details regarding data collection and refinement are given in Table 5. The Enraf–Nonius SDP[45] was used for data collection, and the structures were solved by a combination of MULTAN[46] and successive Fourier differences using either Enraf–Nonius SDP for $Cp_2Mo(dddt)$ or the Xtal3.2 programs[47] for [$Cp_2Mo(dddt)$][TCNQ]. Absorption corrections were applied using empirical procedures based either on the DIFABS algorithm[48] for $Cp_2Mo(dddt)$ or on azimuthal ψ-scans of some reflections having an Eulerian angle χ near 90° (κ > 100°) for [$Cp_2Mo(dddt)$][TCNQ]. H atoms were introduced at calculated positions (C—H, 0.95 Å) except on the outer ethylene bridge of the $dddt^{2-}$ ligand in [$Cp_2Mo(dddt)$][TCNQ] whose carbon atoms exhibit larger thermal agitation factors. The difference Fourier maps failed however to suggest a suitable disorder model for this ethylene group. All atoms were refined anisotropically, except H atoms, which were included in structure factor calculations but not refined. A weighting scheme of the form $w = 1/[\sigma^2(F_o) + 0.0009F_o^2]$ was applied.

Table 5. Crystallographic Data

	$Cp_2Mo(dddt)$	[$Cp_2Mo(dddt)$][TCNQ]
chem form	$C_{14}H_{14}MoS_4$	$C_{26}H_{18}MoN_4S_4$
fw	406.44	610.636
temp, K	293	293
cryst syst	orthorhombic	triclinic
space group (no.)	$Pna2_1$ (33)	P-1 (2)
a (Å)	16.608(3)	9.597(1)
b (Å)	11.568(2)	10.543(4)
c (Å)	7.724(1)	12.460(3)
α (deg)	90.	84.41(2)
β (deg)	90.	80.94(2)
γ (deg)	90.	89.41(2)
V (Å^3)	1483.9(4)	1239.1(5)
Z	4	2
d_{calc} (g cm^{-3})	1.819	1.637
μ (cm^{-1})	14.3	6.98
λ (Å)	0.71079	0.71079
R (F_o)[a]	0.029	0.044
R_w (F_o^2)[b]	0.035	0.058

[a] $R = \sum(||F_o| - |F_c||)/\sum|F_o|$. [b] $R_w = [\sum w(|F_o| - |F_c|)^2/\sum w|F_o|^2]^{1/2}$ with $w = 1/[\sigma^2(F_o) + (0.03F_o^2)^2]$.

Extended Hückel Calculations. The H_{ii} parameters and orbital exponents (ζ) have been taken from ref 18.

Magnetic Studies. Solid-state EPR spectra were recorded on a Varian X-band spectrometer (9.3 GHz) equipped with an Oxford ESR 900 helium cryostat. Susceptibility data were collected on a Quantum Design SQUID at the Physics Department, University of California, Santa Barbara, CA.

Acknowledgment. We thank M.-L. Doublet and E. Canadell, from the Laboratoire de Chimie Théorique (UA CNRS 506), Orsay, France, for stimulating discussions and B. Knight (UCSB) for performing the SQUID measurements. M.F. is indebted to M. and T. Cahuzac for their hospitality during his stay in Bordeaux.

Supporting Information Available: Tables giving atomic coordinates, bond lengths, bond angles, anisotropic thermal parameters, and the least-squares planes for both structures and an ORTEP view with numbering scheme for $TCNQ^{\bullet-}$ in [$Cp_2Mo(dddt)$][TCNQ] (22 pages). Ordering information is given on any current masthead page.

IC950458F

(41) (a) Bashkin, J.; Green, M. L. H.; Poveda, M. L.; Prout, K. *J. Chem. Soc., Dalton Trans.* **1982**, 2485. (b) Green, M. L. H.; McCleverty, J. A.; Pratt, L.; Wilkinson, G. *J. Chem. Soc.* **1961**, 4854. (c) Cooper, R. L.; Green, M. L. H. *J. Chem. Soc. A* **1967**, 1155.
(42) Steimecke, G.; Sieler, H. J.; Kirmse, R.; Hoyer, E. *Phosphorus Sulfur Relat. Elem.* **1979**, *7*, 49.
(43) Schumaker, R. R.; Engler, E. M. *J. Am. Chem. Soc.* **1977**, *99*, 5521.
(44) Larsen, J.; Lenoir, C. *Synthesis* **1989**, 134.
(45) Frenz, B. A. *Enraf-Nonius SDP/Vax Structure Determination Package*, Version 3.0; Enraf-Nonius: Delft, The Netherlands, 1985.
(46) Main, P.; Fiske, S. J.; Hull, S. E.; Lessinger, L.; Germain, G.; Declercq, J. P.; Woolfson, M. M. MULTAN 11/82 A System of Computer Programs for the Automatic Solution of Crystal Structures from X-Ray Diffraction Data. Universities of Louvain, Belgium, and York, England, 1982.
(47) Hall, S. R., Stewart, J. M., Eds. Xtal3.0 Reference Manual. Universities of Western Australia and Maryland, 1990.
(48) Walker, D.; Stuart, N. *Acta Crystallogr.* **1983**, *39A*, 158.